

<https://doi.org/10.22643/JRMP.2019.5.1.18>

Evaluation of ^{99m}Tc -MAG₃-2-nitroimidazole for hypoxic tumor imaging

Yun-Sang Lee*, Young Joo Kim, Jae Min Jeong

Department of Nuclear Medicine, Seoul National University College of Medicine, Seoul, Republic of Korea

ABSTRACT

2-Nitroimidazole derivatives have been reported to accumulate in hypoxic tissue. We prepared a novel ^{99m}Tc -MAG₃-2-nitroimidazole and evaluated the feasibility for hypoxia imaging agent. Bz-MAG₃-2-nitroimidazole was synthesized by direct coupling of Bz-MAG₃ and 2-nitroimidazole using dicyclohexylcarbodiimide. Bz-MAG₃-2-nitroimidazole was labeled with ^{99m}Tc in the presence of tartaric acid and $\text{SnCl}_2 \cdot 2\text{H}_2\text{O}$ at 100°C for 30 min. And the reaction mixture was purified by C₁₈ Sep-pak cartridge. The labeling efficiency and the radiochemical purity were checked by ITLC-SG/acetone/nitrile. The tumor was grown in balb/c mice for 8-13 days after the subcutaneous injection of tumor cells, CT-26 (murine colon adenocarcinoma cell). Biodistribution study and tumor autoradiography were performed in the xenografted mice after i.v injection of 74 kBq/0.1 mL and 19 MBq/0.1 mL of ^{99m}Tc -MAG₃-2-nitroimidazole, respectively. In vivo images of ^{99m}Tc -MAG₃-2-nitroimidazole in tumor bearing mice were obtained 1.5 hr post injection. The labeling efficiency was 45±20% and the radiochemical purity after purification was over 95%. Paper electrophoresis confirmed negative charge of ^{99m}Tc -MAG₃-2-nitroimidazole. ^{99m}Tc -MAG₃-2-nitroimidazole was very stable at room temperature and its protein binding was 53%. The ^{99m}Tc -MAG₃-2-nitroimidazole exhibited high uptake in the liver, stomach and intestine. In biodistribution study using tumor bearing mice, the uptakes (% ID/g) of the tumor were 0.5±0.1, 0.4±0.0, 0.2±0.1 and 0.1±0.1 at 5, 15, 30 min and 4 hrs. Tumor/muscle ratio were 1.4±0.1, 2.2±0.83, 3.0±0.9, and 3.7 (n=2) for 5, 15, 30 min and 4 hrs. The uptake in hypoxic area was found higher than in non-hypoxic area of tumor tissue by autoradiography. In vivo images showed the relatively faint uptake to the hypoxic tumor region. ^{99m}Tc -MAG₃-2-nitroimidazole was successfully synthesized and found feasible for imaging hypoxia.

Key Word: Technetium-99m, 2-Nitroimidazole, MAG₃, Hypoxia, Tumor imaging.

Introduction

Hypoxia, its simple meaning is low oxygen level, especially in solid tumors, it has been recognized for several years to be a potential mechanism of tumor resistance to treatment by radiation and some chemotherapeutic drugs (1-3). Due to the importance of assessment of tumor hypoxia prior to therapy,

there have been many efforts to develop suitable radiopharmaceuticals for imaging tumor hypoxia (4, 5).

The first attempt for targeting of tumor hypoxia was with azomycin, the chemical name is 5-nitroimidazole (6). It is known to be selectively trapped in hypoxia but viable cells because the reduced form of 2-nitroimidazole can be trapped in hypoxia but re-oxidized form of 2-nitroimidazole can come out from

Received: June 17, 2019 / Revised: July 1, 2019 / Accepted: July 5, 2019

Corresponding author : Yun-Sang Lee, Department of Nuclear Medicine, Seoul National University Hospital, 101, Daehak-ro, Jongno-gu, Seoul 03080, Republic of Korea, Tel: +82-2-3668-8906, Fax: +82-745-7690, E-mail: wonza43@snu.ac.kr.

Copyright©2019 The Korean Society of Radiopharmaceuticals and Molecular Probes

normoxia condition in viable cells (3, 6). After then lots so many nitroimidazole derivative have been synthesized and investigated (4, 5). There are two different approaches to developed nitroimidazole derivatives, by direct incorporation of radionuclide and by coupling it with a bifunctional chelating agent. ^{18}F -fluoromisonidazole (^{18}F FMISO) which utilized direct incorporation of ^{18}F fluorine to 2-nitroimidazole was the first extensively investigated as a positron emission tomography (PET) imaging agent (7-10). ^{18}F -fluoroetanidazole (^{18}F FETA), ^{18}F -fluoroerythroimidazole (^{18}F FETNIM) and ^{18}F -labeled EF5, ^{18}F 2-(2-nitro-1[H]-imidazol-1-yl)-N-(2,2,3,3,3-pentafluoropropyl)-acetamide were also reported (10-13). Another 2-nitroimidazole, ^{18}F -fluoroazomycin arabinoside (^{18}F FAZA) and ^{124}I labelled iodoazomycine galactoside (^{124}I IAZG) which utilized direct incorporation were developed as a PET imaging agent (14, 15). But the relatively limited availability of PET facilities, ^{123}I - or $^{99\text{m}}\text{Tc}$ -based radiopharmaceuticals for imaging tumor hypoxia have been developed. ^{123}I -iodoazomycine arabinoside (^{123}I IAZA) which utilized direct incorporation to the modified nitroimidazole is the best studied (16). Oxo[[3,3,9,9-tetramethyl-1-(2-nitro-1H-imidazol-1-yl)-4,8-diazaundecane-2,10-dione dioximato]-(3-)-N,N',N'',N''']technetium (BMS181321) and Oxo[[3,3,9,9-tetramethyl-5-oxa-6-(2-nitro-1H-imidazol-1-yl)-4,8-diazaundecane-2,10-dione dioximato]-(3-)-N,N',N'',N''']technetium (BRU59-21) which utilized coupling nitroimidazole with propylene amineoxime (PnAO) as a bifunctional chelating agent were reported for $^{99\text{m}}\text{Tc}$ labeling ligands (17-20). More recently, $^{99\text{m}}\text{Tc}$ -N-(2'-hydroxybenzyl)-cysteine conjugated metronidazole and ^{68}Ga labeled 2-nitroimidazole derivatives were reported (21, 22).

Mercaptoacetylglycylglycylglycine (MAG_3) is a famous bifunctional chelating agent for $^{99\text{m}}\text{Tc}$ and $^{99\text{m}}\text{Tc}$ - MAG_3 is used in clinic as a renal imaging agent [23-26]. In this, we coupled MAG_3 with 2-nitroimidazole and then labelled MAG_3 -2-nitroimidazole with $^{99\text{m}}\text{Tc}$. And

also we evaluated the physical and biological properties of $^{99\text{m}}\text{Tc}$ - MAG_3 -2-nitroimidazole for confirming of feasibility as a hypoxic tumor imaging agent.

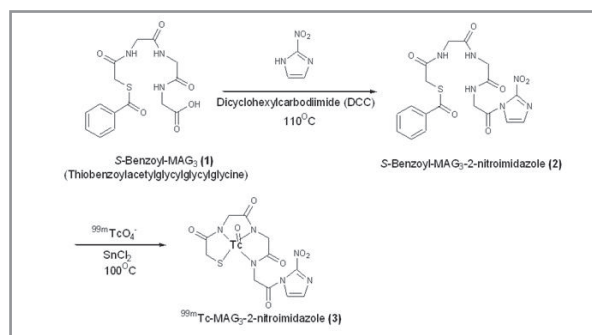
Materials and Methods

1. General

^1H -NMR spectroscopy was recorded on a 300 MHz, AL 300 FT NMR spectrometer (JEOL Ltd., Tokyo, Japan). Mass spectra were obtained using an API-3000 Spectrometer (Applied Biosystems, Foster city, CA, U.S.A.). Thin layer chromatography (TLC) was carried out using pre-coated glass backed silica gel 60 F_{254} TLC plates (E. Merck Company, Darmstadt, Germany) to verify the purity of the products. Kieselgel 60 (230-400 mesh, E. Merck Company, Darmstadt, Germany) was used for silica gel column chromatography. ITLC-SG plates were obtained from the Pall Company (New York, NY, U.S.A.) and Chromatography paper (1 Chr) was obtained from the Whatman International Ltd. (Maidstone, England). A NaI well counter (Packard, Canberra Co., New York, NY, U.S.A.) and a dose calibrator (Atomlab 100, Biodex, New York, NY, U.S.A.) were used to measure the low and high levels of radioactivity, respectively. An AR-2000 TLC Imaging Scanner (Bioscan, Washington DC, U.S.A.) was used to perform the Radio-TLC scan. C_{18} Sep-Pak cartridges were obtained from Waters (Milford, MA, U.S.A.). $^{99\text{m}}\text{Tc}$ -pertechnetate was eluted from the ^{99}Mo - $^{99\text{m}}\text{Tc}$ -generator (Lantheus, MA, U.S.A.) with normal saline. Tissue sections were obtained using cryostat microtome (Leica CM1800, Leica, Germany). Bio-imaging analyzer system (FLA-2000, Fujifilm, Japan) was used for phosphor-imaging study. All cell culture media and reagents were purchased from Invitrogen Inc. (Carlsbad, CA). Other reagents and solvents were purchased from Aldrich, Sigma or Fluka and were used without further purification.

2. Chemical synthesis

Bz-MAG₃-2-nitroimidazole (2) was synthesized by direct coupling of Bz-MAG₃ (1) and 2-nitroimidazole using dicyclohexylcarbodiimide (DCC) (Scheme 1). Bz-MAG₃ (300 mg, 0.81 mmol), 2-nitroimidazole (93 mg, 0.81 mmol) and DCC (171 mg, 0.81 mmol) were kept in a round bottomed flask and DMF (5 mL) was added. The reaction mixture was heated to 120°C and kept for 6 hrs and purified by column chromatography to give Bz-MAG₃-2-nitroimidazole as a yellowish powder (20 mg, 0.043 mmol, 5.3%). ¹H-NMR (300 MHz, D₂O): δ 1.00~1.25 (m, 4H), 1.40~1.75 (m, 4H), 7.57 (t, 2H), 7.71 (t, 1H), 7.92 (d, 2H), 8.37 (d, 1H), 8.51 (d, 1H). MS (ESI, m/z) 457.4 (M⁺+H).



Scheme 1. Synthetic scheme of ^{99m}Tc-MAG₃-2-nitroimidazole.

3. ^{99m}Tc labeling

1 mg of Bz-MAG₃-2-nitroimidazole was dissolved in 0.25 mL of 0.01 M sodium hydroxide, and then tartaric acid (40 mg), lactose (20 mg) and SnCl₂·2H₂O (0.4 mg/0.4 mL of 0.02 M HCl) were added. Final pH of the mixture was adjusted to 5 with 10 M sodium hydroxide. After adding the freshly eluted ^{99m}Tc-pertechnetate (370-555 MBq/4 mL), the reaction mixture was incubated at 100°C for 30 min (Scheme 1). Crude ^{99m}Tc-MAG₃-2-nitroimidazole was purified by C₁₈ Sep-Pak cartridge and 40% EtOH in water as eluent. The

labeling efficiency and the radiochemical purity were checked by ITLC-SG (10 × 100 mm) as a stationary phase and acetonitrile as a mobile phase.

4. Stability of ^{99m}Tc-MAG₃-2-nitroimidazole

We checked the stability of ^{99m}Tc-MAG₃-2-nitroimidazole at room temperature and at 37°C in human serum albumin. 0.1 mL of ^{99m}Tc-MAG₃-2-nitroimidazole was incubated either at room temperature or at 37°C after mixing with human serum (1 mL). The stability was checked by TLC (ITLC-SG/acetonitrile) at 15, 30 min, 1, 2, 4 and 6 hr after incubation.

5. Serum protein binding of ^{99m}Tc-MAG₃-2-nitroimidazole

To confirm the possibility of non-specific binding, we checked the protein binding. Human blood sample was placed into a glass tube and centrifuged. 1 mL of human serum was mixed with ^{99m}Tc-MAG₃-2-nitroimidazole (13 MBq/0.1 mL) and then incubated at 37°C. After 15, 30 min, 2, 4 and 6 hr, 200 μL of aliquots were put into centrifugal filter units (Ultrafree-MC, Millipore Co., Bedford, MA), and centrifuged at 15,000 rpm for 10 min. The 50 μL aliquots of the filtrates and original samples were separately placed into a test tube and the radioactivities were counted with a NaI well counter. The percentages of the protein bound form were calculated as follows:

$$\text{Protein binding (\%)} = \frac{(\text{1-cpm of filtrate/cpm of original sample}) \times 100}{1}$$

6. Paper electrophoresis of ^{99m}Tc-MAG₃-2-nitroimidazole

We performed paper electrophoresis for confirming the charge of ^{99m}Tc-MAG₃-2-nitroimidazole. Whatman chromatography paper was cut (1×10 cm) and soaked

with a 0.2 M sodium phosphate buffer (pH 8.0). The paper was set to the horizontal electrophoresis device and 0.2 M sodium phosphate buffer (pH 8.0) was placed in the tanks. After loading the labeled samples at the center of the papers, DC electricity (100 V) was supplied for 1 hr. The papers were then removed from the device and scanned using a Radio-TLC scanner.

7. Biodistribution

Murine colon adenocarcinoma cell line (CT-26) was obtained from Korean Cell Line Bank (Seoul, Korea). CT-26 cells were grown in DMEM medium supplemented with 10% heat inactivated fetal bovine serum and ampicillin/streptomycin. Cell line was maintained in a humidified 5% CO₂ atmosphere at 37°C. Animal study was carried out in compliance with the local institutional regulations. Balb/c mice (male, 3-4 week old) were xenografted with CT-26 cell line by implanting 5×10⁶ cells subcutaneously in their left thighs. The tumors were allowed to grow for 8-13 days. 0.1 mL of ^{99m}Tc-MAG₃-2-nitroimidazole (74 kBq) was injected to the tumor bearing mice (20±1 g, n=3/group) through the tail vein. The mice were sacrificed by cervical dislocation after 5, 15, 30 min and 4 and 19 hr. Blood, tumor and other organs were rapidly separated and weighed. The radioactivities of the samples were counted with a NaI well counter. Results were expressed as percentage of injected dose per gram of tissue (% ID/g).

8. Tissue section images of tumor

To confirm that the hot uptake region was real hypoxic zone or not, we performed the phosphorimaging and H&E staining of tumor tissue. ^{99m}Tc-MAG₃-2-nitroimidazole (18 MBq/0.1 mL) was injected to the mouse bearing CT-26 xenografts (male, about

20g) through the tail vein. After 15 min, mouse was sacrificed by cervical dislocation. Tumor was quickly excised and frozen at -20°C, and was cut into 7 or 20 μm sections on a cryostat. For phosphorimaging study, 20 μm sections were exposed to the imaging plate of a Bio-imaging analyzer system (BAS). The histologic structures in each set of sections were identified from the adjacent 7 μm section stained with hematoxylin and eosin (H&E).

9. Gamma camera imaging of mice

We took the images of the tumor bearing mouse (male, balb/c mouse, 20 g) with ^{99m}Tc-MAG₃-2-nitroimidazole. The tumor size was almost 20 mm. Gamma camera was equipped with a low energy pinhole (4 mm) collimator. 27.4 MBq of ^{99m}Tc-MAG₃-2-nitroimidazole was injected into a tumor bearing mouse through the tail vein. Planar images of the mouse in prone position with shielding the abdominal region were obtained after 1.5, 3 and 4 hr.

Results and discussion

1. Chemical synthesis and ^{99m}Tc-labeling

Bz-MAG₃-2-nitroimidazole (2) was synthesized by direct coupling of Bz-MAG₃ (1) and 2-nitroimidazole and purified by column chromatography. The chemical structure of Bz-MAG₃-2-nitroimidazole was confirmed by ¹H-NMR and mass spectrometry. Labeling efficiency and radiochemical purity were checked by ITLC-SG/acetonitrile. The R_f value of ^{99m}Tc-MAG₃-2-nitroimidazole was 0.5, and both of the R_f values of ^{99m}Tc-MAG₃ and ^{99m}Tc-colloid were determined to be around 0. The R_f value of ^{99m}Tc-pertechnetate was determined to be 1. The labeling efficiency was 45±20% (Fig. 1. A). Due to impurities of the crude

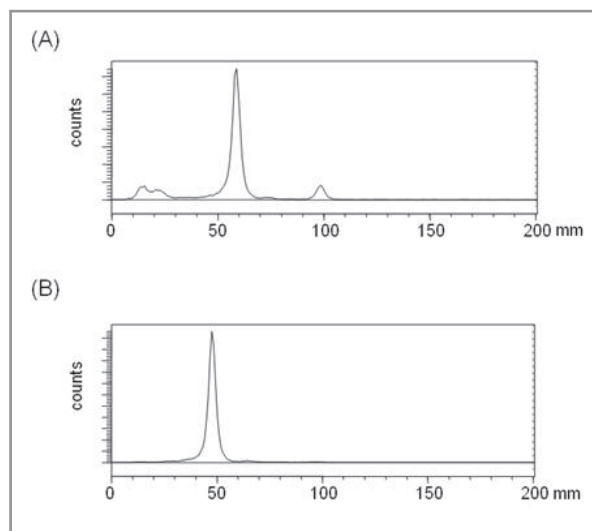


Figure 1. Chromatograms of crude ^{99m}Tc -MAG₃-2-nitroimidazole (A) and the purified ^{99m}Tc -MAG₃-2-nitroimidazole (B) with C₁₈ Sep-Pak cartridge. Chromatography was performed on ITLC-SG (10 × 100 mm) /acetonitrile.

^{99m}Tc -MAG₃-2-nitroimidazole preparation, purification step was needed to use *in vitro* and *in vivo* studies. After purification with C₁₈ Sep-Pak cartridge, the radiochemical purity of ^{99m}Tc -MAG₃-2-nitroimidazole was over 95% (Fig. 1. B).

2. The stability of ^{99m}Tc -MAG₃-2-nitroimidazole

The stability of ^{99m}Tc -MAG₃-2-nitroimidazole was checked by radio-TLC and found to be stable at least for 6 hr at room temperature. However, in human serum at 37°C, the radiochemical purity of ^{99m}Tc -MAG₃-2-nitroimidazole decreased to 55% after 6 hours (Fig. 2).

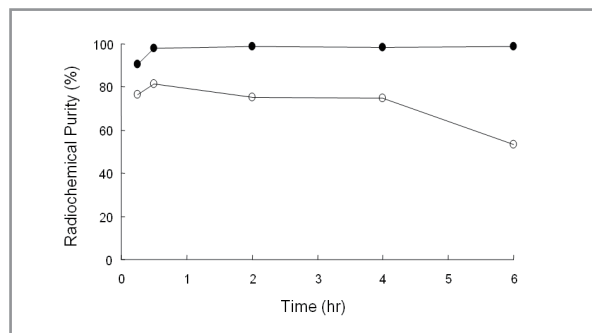


Figure 2. Stability of ^{99m}Tc -MAG₃-2-nitroimidazole at room temperature (●) and in human serum at 37°C (○).

3. Serum protein binding and paper electrophoresis of ^{99m}Tc -MAG₃-2-nitroimidazole

The percentage of protein binding of ^{99m}Tc -MAG₃-2-nitroimidazole was showed high until 6 hr. At 15 min after incubation with human serum, the percentage of protein binding was over 98%. In paper electrophoresis experiment, ^{99m}Tc -MAG₃-2-nitroimidazole moved slightly to the anode (Fig. 3). This result indicated that ^{99m}Tc -MAG₃-2-nitroimidazole has a negative charge as we

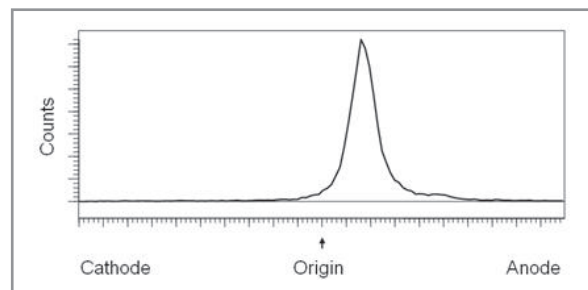


Figure 3. Paper electrophoresis of ^{99m}Tc -MAG₃-2-nitroimidazole using 0.2 M sodium phosphate buffer (pH 8.0) at 100 V for 1 hr.

expected.

4. Biodistribution

Biodistribution experiments were performed on tumor bearing mice. ^{99m}Tc -MAG₃-2-nitroimidazole exhibited high uptakes in the liver, stomach and intestine (Table 1). The tumor uptake of ^{99m}Tc -MAG₃-2-nitroimidazole was decreased by time until 19 hrs post injection. The tumor to muscle ratio were 1.4, 2.2, 3.0 and 3.7 for 5, 15, 30 min and 4 hrs, respectively. Tumor uptake of ^{99m}Tc -MAG₃-2-nitroimidazole was not so high throughout the whole time to 19 hrs, and the highest uptake was 0.5 ± 0.1 %ID/g at 5 min after the ^{99m}Tc -MAG₃-2-nitroimidazole injection. Low tumor uptake of ^{99m}Tc -MAG₃-2-nitroimidazole may due to the high protein binding of ^{99m}Tc -MAG₃-2-nitroimidazole and its fast uptake to the liver and ^{99m}Tc -

Table 1. Biodistribution of ^{99m}Tc -MAG₃-2-nitroimidazole after intravenous administration in tumor bearing mice.

Tissue	^{99m}Tc -MAG ₃ -2-nitroimidazole				
	5 min	15 min	30 min	4 hr	19 hr
Blood	3.6±0.7	1.7±0.1	0.3±0.1	0.1±0.0	0.1±0.1
Muscle	0.4±0.1	0.2±0.1	0.1±0.0	0.0±0.0	0.0±0.0
Fat	1.2±0.2	0.8±0.1	0.4±0.2	0.0±0.0	0.0±0.0
Heart	1.0±0.2	0.5±0.0	0.1±0.0	0.1±0.0	0.0±0.0
Lung	2.6±0.5	1.3±0.1	1.2±1.7	0.2±0.3	0.1±0.1
Liver	70.0±5.2	39.4±4.6	16.9±10.7	5.2±2.1	0.3±0.0
Spleen	1.3±0.3	0.9±0.3	0.4±0.1	0.2±0.1	0.0±0.0
Stomach	37.9±14.6	145.6±29.0	87.4±22.5	9.1±1.4	0.1±0.1
Intestine	20.3±1.2	38.6±4.4	47.8±10.6	62.5±8.5	0.1±0.0
Kidney	25.2±5.8	8.3±1.9	2.9±0.7	0.5±0.2	0.1±0.0
Brain	0.6±0.8	0.1±0.0	0.0±0.0	0.1±0.0	0.0±0.0
Bone	0.7±0.1	0.4±0.1	0.7±0.7	0.0±0.0	0.0±0.0
Tumor	0.5±0.1	0.4±0.0	0.2±0.1	0.1±0.1	0.0±0.0

^a Expressed as % ID/g and mean ± SD (n = 3/group)

MAG₃-2-nitroimidazole is rapidly metabolized to free ^{99m}Tc (high stomach uptake) and other hydrophilic metabolites (high kidney uptake).

5. Tissue section images of tumor

Phosphor images and histopathologic images of the adjacent tumor sections were obtained (Fig. 4). Even though the low tumor uptake in the biodistribution study, the uptake of ^{99m}Tc -MAG₃-2-nitroimidazole in hypoxic area was found higher than in non-hypoxic area of tumor tissue by the autoradiography and H&E staining comparison. High signal from ^{99m}Tc -MAG₃-2-nitroimidazole in the autoradiography is well matched with the cell death in the hypoxic tissue from the H&E staining result.

6. Gamma camera imaging of mice

Figure 5 showed that ^{99m}Tc -MAG₃-2-nitroimidazole

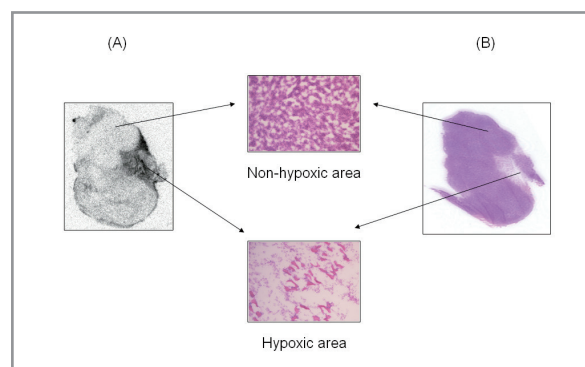


Figure 4. Phosphor image (A) and histopathologic images (B) of the tumor sections from ^{99m}Tc -MAG₃-2-nitroimidazole injected mice.

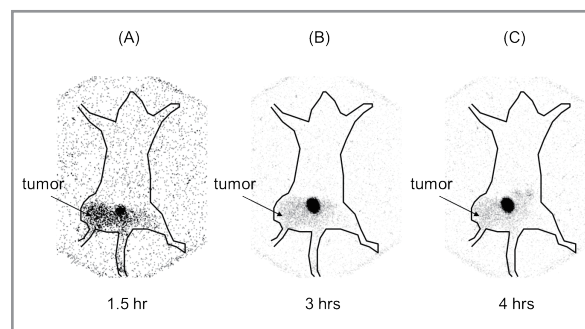


Figure 5. Imaging 1.5 (A), 3 (B) and 4 hr (C) after injection of ^{99m}Tc -MAG₃-2-nitroimidazole in tumor bearing mouse.

was relatively high uptake by tumor. The 1.5 hr image was the highest tumor uptake among three images. To get high contrast image, we covered the abdominal and brain area with a lead panel and the stomach and intestine uptake were not shown in these images which were confirmed in biodistribution study. Even though the highest uptake of ^{99m}Tc -MAG₃-2-nitroimidazole is 0.5 ± 0.1 %ID/g at 5 min after the injection and the uptake in the tumor site decreased to last of time points, we waited for 1.5 hr to reduce the bladder signal. High bladder uptake due to the rapid degradation of ^{99m}Tc -MAG₃-2-nitroimidazole in the liver and hydrophilic metabolites generation.

Conclusion

We have successfully synthesized ^{99m}Tc -MAG₃-2-nitroimidazole. Biodistribution and autoradiography study showed it bound selectively to hypoxic cells on CT26 tumor tissues. In vivo images showed the faint uptake to the hypoxic tumor region. This image result was not so satisfactory, however, we could find the feasibility of ^{99m}Tc -MAG₃-2-nitroimidazole for hypoxic tumor imaging agent.

Acknowledgments

This work was carried out by the research fund supported by Radiation Technology R&D program (NRF-2017M2A2A7A01021401) through the National Research Foundation of Korea (NRF). The authors declare no conflict of interest.

References

1. Gray LH, Conger AD, Ebert M, Hornsey S, Scott OC. The concentration of oxygen dissolved in tissues at the time of irradiation as a factor in radiotherapy. *Br J Radiol* 1953;26:638-648.
2. Moulder JE, Rockwell S. Tumor hypoxia: its impact on cancer therapy. *Cancer Metastasis Rev* 1987;5:313-341.
3. Chapman JD, Urtasun RC, Blakely EA, Smith KC, Tobias CA. Hypoxic cell sensitizers and heavy charged-particle radiations. *Br J Cancer Suppl* 1978;37:184-188.
4. Nunn A, Linder K, Strauss HW. Nitroimidazoles and imaging hypoxia. *Eur J Nucl Med* 1995;22:265-280.
5. Ballinger JR. Imaging hypoxia in tumors. *Semin Nucl Med* 2001;31:321-329.
6. Webster LT. Drugs used in chemotherapy of protozoal infections. In: Gilman AG, Rall TW, Nies AS, Taylor P. eds. The pharmacological basis of therapeutics. 8th edn. New York. *Pergamon* 1990:1002-4
7. Koh WJ, Rasey JS, Evans ML, Grierson JR, Lewellen TK, Graham MM, Krohn KA, Griffin TW. Imaging of hypoxia in human tumors with [F-18] fluoromisonidazole. *Int J Radiat Oncol Biol Phys* 1992;22:199-212.
8. Valk PE, Mathis CA, Prados MD, Gilbert JC, Budinger TF. Hypoxia in human gliomas: demonstration by PET with fluorine-18-fluoromisonidazole. *J Nucl Med* 1992;33:2133-2137.
9. Yeh SH, Liu RS, Wu LC, Yang DJ, Yen SH, Chang CW, Yu TW, Chou KL, Chen KY. Fluorine-18 fluoromisonidazole tumour to muscle retention ratio for the detection of hypoxia in nasopharyngeal carcinoma. *Eur J Nucl Med* 1996;23:1378-1383.

10. Rasey JS, Hofstrand PD, Chin LK, Tewson TJ. Characterization of [¹⁸F]fluoroetanidazole, a new radiopharmaceutical for detecting tumor hypoxia. *J Nucl Med* 1999;40:1072-1079.
11. Yang DJ, Wallace S, Cherif A, Li C, Gretzer MB, Kim EE, Podoloff DA. Development of F-18-labeled fluoroerythronitroimidazole as a PET agent for imaging tumor hypoxia. *Radiology* 1995;194:795-800.
12. Gronroos T, Eskola O, Lehtio K, Minn H, Marjamaki P, Bergman J, Haaparanta M, Forsback S, Solin O. Pharmacokinetics of [¹⁸F]FETNIM: a potential marker for PET. *J Nucl Med* 2001;42:1397-1404.
13. Dolbier WR Jr, Li AR, Koch CJ, Shiue CY, Kachur AV. [¹⁸F]-EF5, a marker for PET detection of hypoxia: synthesis of precursor and a new fluorination procedure. *Appl Radiat Isot* 2001;54:73-80.
14. Piert M, Machulla HJ, Picchio M, Reischl G, Ziegler S, Kumar P, Wester HJ, Beck R, McEwan AJ, Wiebe LI, Schwaiger M. Hypoxia-specific tumor imaging with ¹⁸F-fluoroazomycin arabinoside. *J Nucl Med* 2005;46:106-113.
15. Zanzonico P, O'Donoghue J, Chapman JD, Schneider R, Cai S, Larson S, Wen B, Chen Y, Finn R, Ruan S, Gerweck L, Humm J, Ling C. Iodine-124-labeled iodo-azomycin-galactoside imaging of tumor hypoxia in mice with serial microPET scanning. *Eur J Nucl Med Mol Imaging* 2004;31:117-128.
16. Mannan RH, Somayaji VV, Lee J, Mercer JR, Chapman JD, Wiebe LI. Radioiodinated 1-(5-iodo-5-deoxy-beta-D-arabinofuranosyl)-2-nitroimidazole (iodoazomycin arabinoside: IAZA): a novel marker of tissue hypoxia. *J Nucl Med* 1991;32:1764-1770.
17. Linder KE, Chan YW, Cyr JE, Malley MF, Nowotnik DP, Nunn AD. TcO(PnA.O-1-(2-nitroimidazole)) [BMS-181321], a new technetium-containing nitroimidazole complex for imaging hypoxia: synthesis, characterization, and xanthine oxidase-catalyzed reduction. *J Med Chem* 1994;37:9-17.
18. Ballinger JR, Kee JW, Rauth AM. In vitro and in vivo evaluation of a technetium-99m-labeled 2-nitroimidazole (BMS181321) as a marker of tumor hypoxia. *J Nucl Med* 1996;37:1023-1031.
19. Johnson LL, Schofield L, Mastrofrancesco P, Donahay T, Nott L. Technetium-99m-nitroimidazole uptake in a swine model of demand ischemia. *J Nucl Med* 1998;39:1468-1475.
20. Melo T, Duncan J, Ballinger JR, Rauth AM. BRU59-21, a second-generation ^{99m}Tc-labeled 2-nitroimidazole for imaging hypoxia in tumors. *J Nucl Med* 2000;41:169-176.
21. Das T, Banerjee S, Samuel G, Sarma HD, Korde A, Venkatesh M, Pillai MR. ^{99m}Tc-labeling studies of a modified metronidazole and its biodistribution in tumor bearing animal models. *Nucl Med Biol* 2003;30:127-134.
22. Hoigebazar L, Jeong JM, Choi SY, Choi JY, Shetty D, Lee YS, Lee DS, Chung JK, Lee MC, Chung YK. Synthesis and characterization of nitroimidazole derivatives for ⁶⁸Ga-labeling and testing in tumor xenografted mice. *J Med Chem* 2010;53:6378-6385.
23. Fritzberg AR, Kasina S, Eshima D, Johnson DL. Synthesis and biological evaluation of technetium-99m MAG₃ as a hippuran replacement. *J Nucl Med* 1986;27:111-116.
24. Eshima D, Fritzberg AR, Taylor A Jr. ^{99m}Tc renal tubular function agents: current status. *Semin Nucl Med* 1990;20:28-40.
25. Eshima D, Taylor A Jr. Technetium-99m (^{99m}Tc) mercaptoacetyltriglycine: update on the new ^{99m}Tc renal tubular function agent. *Semin Nucl Med* 1992;22:61-73.
26. Itoh K. ^{99m}Tc-MAG₃: review of pharmacokinetics, clinical application to renal diseases and quantification of renal function. *Ann Nucl Med* 2001;15:179-190.